Fizika Nizkikh Temperatur, 1996, v. 22, No 2, p. 194–204

Thermal conductivity of solid oxygen, nitrogen, and their solid solutions

Yu. A. Freiman[1], A. Jeżowski[2], P. Stachowiak[2], V. V. Sumarokov[1], and J. Mucha[2]

[1] *B. Verkin Institute for Low Temperature Physics & Engineering, National Academy of Sciences of Ukraine 47 Lenin Ave., 310164 Kharkov, Ukraine*
E-mail:freiman@ilt.kharkov.ua

[2] *W. Trzebiatowski Institute for Low Temperatures and Structure Research, Polish Academy of Sciences PO Box 937, 50-950 Wroclaw 2, Poland*

1. Introduction

Solid oxygen and nitrogen belong to the group of molecular crystals formed by linear molecules. These solids except for rare-gas solids are the simplest crystals with regard to crystal structure, lattice dynamics, and other physical properties. During the last three decades, most of the physical properties of these solids at equilibrium vapor pressure have been studied rather thoroughly (see, e.g., [1,2]). Thermal conductivity seems to be the only exception.

Among many binary solutions of cryocrystals (solidified noble gases and simple molecular crystals) one of the most interesting in many respects is the N_2-O_2 system. It is due not only to the specific position which the elements hold in the nature, but also to the peculiar character of the oxygen molecule and the unique magnetic properties of solid oxygen.

In this paper we report results of the first measurements of the thermal conductivity of solid oxygen, the low-temperature thermal conductivity of solid nitrogen and O_2-N_2 solid solutions. Preliminary data on pure solids have been published in Refs. 3,4.

Investigation of the thermal conductivity imposes high demands upon the sample quality. The large jump in the volume at the phase transformations in solid O_2 and N_2 makes practically impossible obtaining single crystals of the low temperature phases of these crystals. Even growing of high quality polycrystals presents a considerable challenge to the experimenters. That is why the studies of thermal conductivity were never performed for the two low-temperature phases of solid oxygen and for the low-temperature range in the case of solid nitrogen. The sole measurement of the thermal conductivity of solid O_2 was done for a single point at 48 K in the gamma phase [5]. The thermal conductivity of solid nitrogen was studied before from the triple point down to 20 K [6,7].

The measurements described in this paper have been made possible due to the crystal growth method developed specially for the crystals having a great jump in volume during the phase transitions in the solid state. The method, which made it possible to obtain samples free from visible cracks and defects, was originally developed and tested on solid oxygen [3] and then used for solid nitrogen and their solid solutions. The method is based on the comprehensive study by Prikhotko et al. [8] of the influence of growth conditions upon the quality of samples of solid oxygen. It was shown that the number of nucleation centers of the β phase could be reduced significantly by slowing down the rate of passing through the $\gamma-\beta$ transition and by annealing the samples just below the transition point which gives rise to amalgamation of grains close in orientation and growing some of them at the expence of others. The authors reported that they managed to grow single crystals of the β phase as large as 0.2–0.4 mm and the crystals did not crack during the subsequent cooling through the transition.

2. Solid oxygen

In the present study the samples of solid oxygen were grown from the melt with the velocity of the solidification front of ~1 mm/h. The samples were annealed slightly below the triple point for about 6 h.

As a result we obtained transparent single crystals of γ-oxygen. The rate of cooling from T_{tr} to the $\gamma-\beta$ transformation point was 1 K/h. The total time of the $\gamma-\beta$ transition passage was about 100 h. The cooling rate of β-oxygen was 1.5 K/h. The region of the $\beta-\alpha$ transition was traversed during 5 h. The samples of

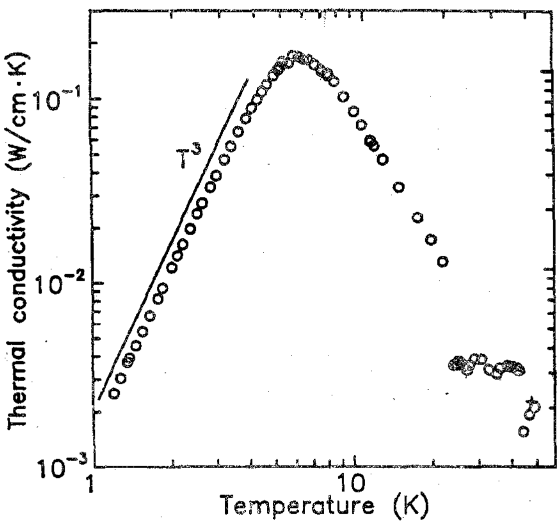

Fig. 1. Thermal conductivity of solid oxygen as a function of temperature.

α- and β-oxygen were transparent without visible defects, though slightly cloudy.

Results of the measurements of the thermal conductivity κ in the α, β, and γ phases of solid oxygen are given in Fig. 1. As one can see, the temperature dependence of the thermal conductivity in the α phase is typical of an insulator, with a maximum around 6 K. The magnitude of the thermal conductivity at the maximum (approximately 0.17 W/(cm·K)) is nearly the same as the maximum thermal conductivity of the classical rare gas solids like Ar and Kr [9], and close to the value for solid nitrogen (see [4] and Sec. 4). However, it is distinctly lower as compared to the maximum thermal conductivity of quantum solids like He [9] and H_2 [10].

The most intriguing feature is the jump in the thermal conductivity of solid oxygen at the $\alpha-\beta$ transition point, the decrease in κ amounting to 70%. It should be stressed that the data are not only reversible with respect to the direction of temperature variation but also reproducible from run to run and from sample to sample.

In the β phase the thermal conductivity only slightly decreases with rising temperature. The temperature dependence can be represented by the equation $\kappa = (3.92-0.0117\,T)\cdot 10^{-3}$ W/(cm·K). The total change of the thermal conductivity over the temperature range of existence of the β phase is ~10%. At the $\beta-\gamma$ transition point, the thermal conductivity drops by 60%.

In the γ phase the thermal conductivity increases nearly linearly with temperature. A similar behavior of the thermal conductivity for so-called plastic phases was observed in molecular crystals [5] and can be understood if we take into account that both the molecular rotation is becoming progressively less hindered and the magnetic correlation length is decreasing with rising temperature.

We explained [3] the observed anomalies in the following way. In the magnetically ordered α phase the total thermal conductivity is the sum of a phonon thermal conductivity κ_{ph} and a magnon contribution κ_m, whereas the librons, owing to a large gap in their energy spectrum, contribute mostly to the scattering mechanisms. The main contribution to the magnon thermal conductivity comes from the lower magnon mode with the quasi-2D energy spectrum. Our estimates show that the magnon heat transport may be a considerable part of the total heat transport. As the temperature is raised the magnons gradually start to contribute to the scattering as well and, upon reaching the $\alpha-\beta$ transition, the upper magnon mode of 27 cm^{-1} will take part both in the scattering and in heat transport.

The anomalous character of $\kappa(T)$ in the β phase (Fig. 1) is a consequence of the anomaly in the temperature dependences of the sound velocities [11] which in turn is a result of an unusually high magnetoelastic coupling in solid oxygen. According to [11], the sound velocities increase with temperature throughout nearly the entire range of existence of β-oxygen, the increase reaching 30% in the case of the transverse sound. But the phonon mean free path, calculated with account of the sound velocity [11], the molar volume [12], and lattice heat capacity [13] data, reveals the «normal» (for this temperature range) temperature dependence.

As none of the measured thermodynamic characteristics shows a jump at the $\alpha-\beta$ transition point, we have originally [3] tied the observed jump of the thermal conductivity to the magnon component of the heat transport. Upon the transition to the magnetically disordered β phase this contribution naturally disappears, giving rise to the jump.

Measurements of the thermal conductivity in high magnetic field, which shifts positions of the magnon modes and at the same time does not disturb the phonon modes, could shed light on the nature of the jump and, generally, verify the hypothesis of the magnetic origion of the anomalies in the thermal conductivity.

There exists another approach to this problem. It involves doping solid oxygen with nonmagnetic impurities. Such impurities tend to damp and shift the magnon modes which will influence the magnon contribution to thermal conductivity.

3. Solid oxygen doped with nonmagnetic impurities

We took N_2 and Ar as nonmagnetic impurities which have parameters ε and σ of the Lennard—Jones intermolecular potential close to those of oxygen. As it follows from the phase diagrams of the O_2–N_2 [14] and O_2–Ar [15] solid solutions, the solubility of N_2 does not exceed 1% in α-O_2 and 2% in β-O_2. The solubility of Ar in α-O_2 does not exceed 2%; in the β phase near the α–β transition point the solubility increases to 5%, falling to 2% with increasing temperature.

Far-infrared absorption spectra of the solid solutions allow one to get information about the effect of impurities on magnon modes. Such investigations have been performed on the O_2–N_2 [16] and O_2–Ar systems [17]. Unfortunately, information presented in these works seems to be incomplete, and, besides, concerns only the upper magnon mode. In particular, it was shown [17] that the increase of the Ar concentration in the sample up to 1% had no tangible effect on the frequency of the magnon mode. However, the intensity of the mode decreased 2.5 times, and its halfwidth increased more than twice compared to the respective values for pure oxygen. The intensity of the magnon mode in doped samples declined with increasing temperature more rapidly than in nondoped ones, and above 20 K the mode became unobservable.

Thus, it should be expected that doping solid oxygen with impurities will influence the thermal

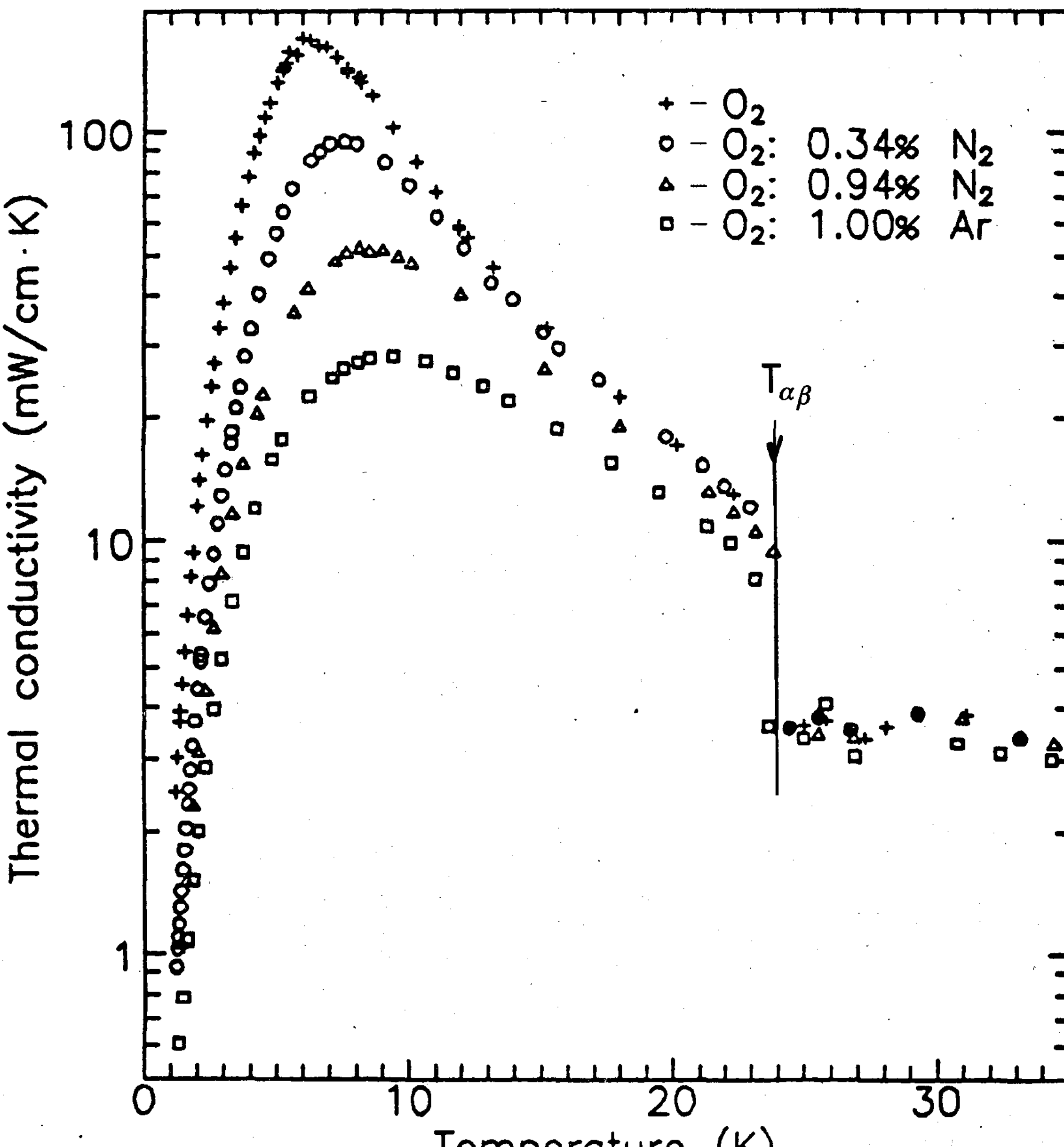

Fig. 2. Temperature dependence of the thermal conductivity of pure oxygen and O_2–N_2 and O_2–Ar solid solutions.

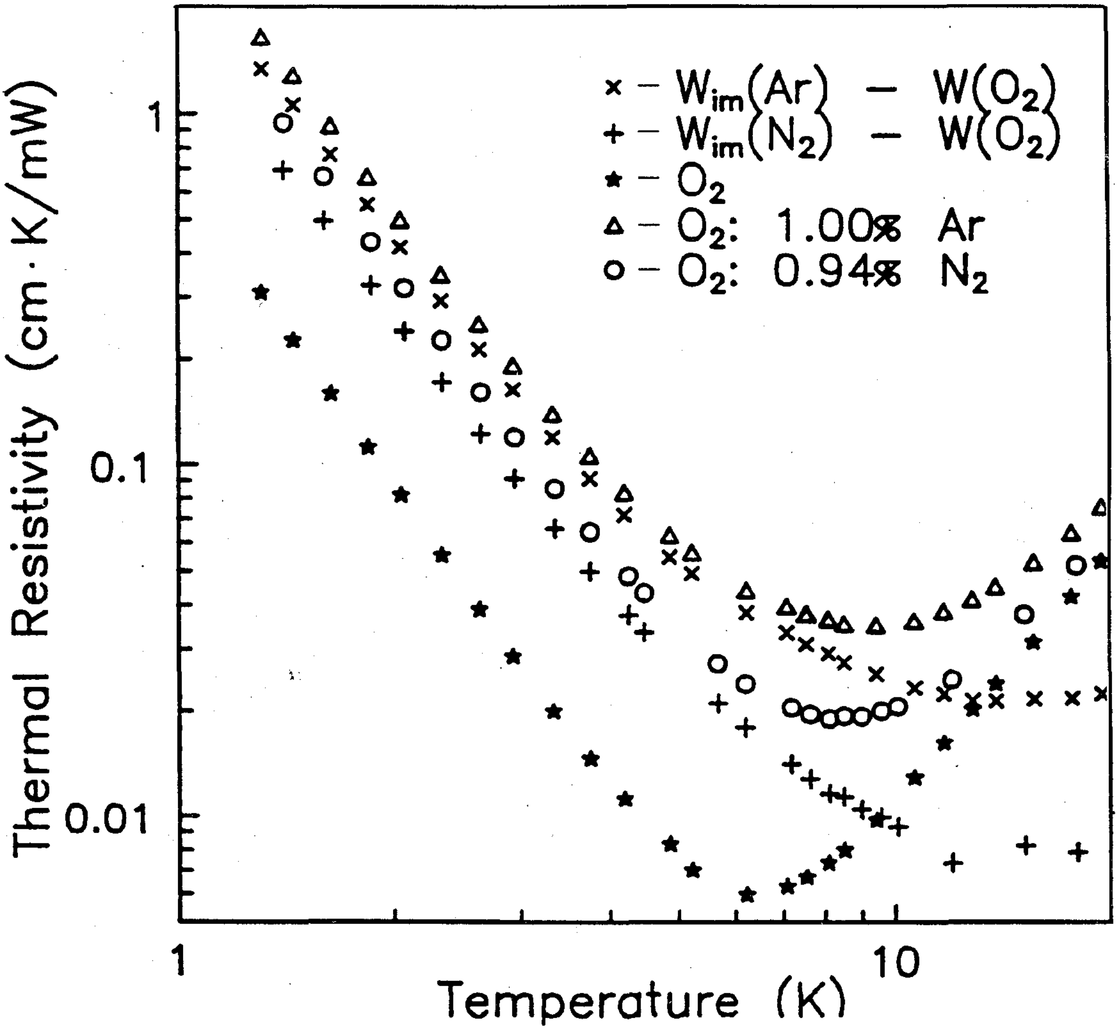

Fig. 3. Comparison of the thermal resistivity of the solid solutions O_2-N_2 and O_2-Ar with the total resistivity of pure solid oxygen and the N_2-O_2 solution.

conductivity considerably stronger than in the case of nonmagnetic molecular crystals.

In this Section we report the thermal conductivity of O_2-N_2 (0.34% and 0.94% N_2) and $O_2-1\%$ Ar solid solutions measured in the temperature range 1–35 K.

The purity of the investigated substances was 99.9% (main impurity 0.01% CO_2) for O_2; 99.9995% (main impurity O_2) for N_2; 99.995% (main impurities: O_2 and N_2) for Ar.

Gaseous mixtures for the samples were prepared by the *PVT* method. Composition analysis of the sample was performed before and after measurements by means of a mass spectrometer. The error of the composition determination did not exceed 0.01%. The conditions of crystal growth and the sample cooling rate were the same as for pure oxygen. The random error of the measurements did not exceed 3%.

The experimental data obtained are shown in Figs. 2–4. Figure 2 presents the temperature dependence of the thermal conductivity for pure solid oxygen [1] and for the solid solutions $O_2-0.34\%$ N_2; $O_2-0.94\%$ N_2; and $O_2-1\%$ Ar.

The data for the $O_2-0.94\%$ N_2 and $O_2-1\%$ Ar solid solutions are shown in Fig. 3 as plots of ΔW vs T where ΔW is the excess thermal resistivity obtained by subtracting the thermal resistivity of pure oxygen from the values for solid solutions.

Figure 4 shows the temperature dependence of $\Delta W/W(O_2)$ (the reduced thermal resistivity) for the solid solutions studied. The analogous quantity $\Delta W/W(N_2)$ for the $N_2-1.12\%$ O_2 system is shown for comparison. To compare the data relating to different concentrations c the curves were normalized to the impurity fractions expressed in percent.

The thermal conductivity versus T curves for all the solid solutions studied, as well as for pure oxygen, exhibit well-defined maxima (Fig. 2). Doping with

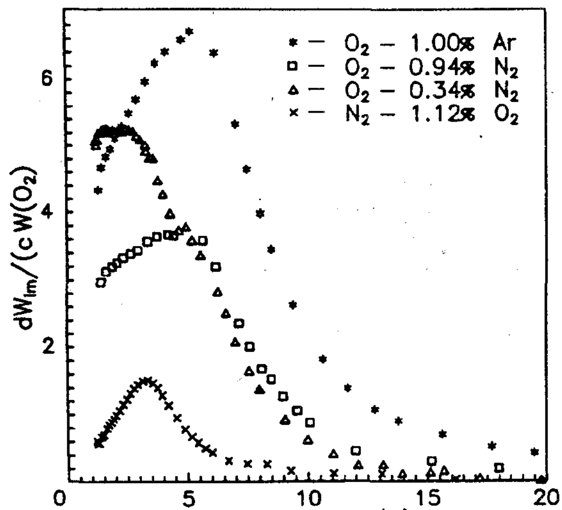

Fig. 4. Comparison of temperature dependences of the reduced excess thermal resistivity of solid solutions O_2–Ar, O_2–N_2, and N_2–O_2, normalized to 1% of admixture.

impurities leads to a considerable decrease and widening of the maxima, and shifts the maxima towards higher temperatures. All the effects are appreciably stronger for doped solid oxygen than for doped solid nitrogen (see Sec. 5). Doping O_2 with 1% of Ar results in a more than 3 K shift of the thermal conductivity maximum relative to its position for pure oxygen; in the case of O_2–0.94%N_2 it amounts to 2.5 K. On the other hand, in the case of N_2–1.12% O_2 the shift does not exceed 0.4 K.

Examination of Figs. 2 and 3 reveals that in the low temperature region the excess thermal resistivity of solid solutions exceeds the thermal resistivity of the matrix, i.e. scattering of the thermal flow on impurities turns out to be the main cause of the thermal resistance. The maximum value of $\Delta W/(cW(O_2))$ for nitrogen-doped solid O_2 is more than twice (in the case of O_2–1% Ar, more than four times) as that for solid N_2 doped with oxygen.

The low temperature thermal conductivities ($T < 3.4$ K) can be described as a power law of the form $\kappa \sim T^{\delta}$. The exponent δ, which is in general a function of the impurity concentration, turned out to be the same as for pure oxygen and for the solid solutions containing 0.34% and 0.94 % N_2. As a result, the curves $\Delta W/W(O_2)$ (Fig. 4) contain nearly horizontal sections in the low temperature range. It is the range where, according to our estimates [3], the magnon contribution to the heat transport of pure oxygen is considerable. This contribution can be roughly estimated from the data of Fig. 4. The total thermal conductivity is the sum of a phonon thermal conductivity κ_{ph} and a magnon contribution κ_m. Assuming that in the solid solution studied the magnon contribution is suppressed and taking the value of $\kappa^0_{ph}/\kappa_{ph}$ for the solid solution N_2–1.12% O_2 from Fig. 4, we arrive at the estimated ratio maximum $\kappa^0_m/\kappa^0_{ph} \sim 2$ (κ^0_m, κ^0_{ph} are the values for pure solid oxygen) which is in agreement with our previous estimates [3].

In the low temperature range the effect of doping is essentially nonlinear in concentration. However, at $T \gtrsim 5$ K the effect is approximately linear with N_2 concentration. As the temperature increases, the relative value of the impurity effect decreases. For the O_2–0.34% N_2 solid solution the effect becomes insignificantly small above 18 K, but for the solutions O_2–0.94% N_2 and O_2–1% Ar the influence of impurities is distinctly observable up to the $\alpha-\beta$ transition.

The two most unexpected effects found are: (1) persistence of the thermal conductivity jump at the $\alpha-\beta$ transition in the presence of impurities and (2) insensitivity of the thermal conductivity in the β phase to the presence of impurities (Figs. 1, 2). Although the value of the jump depends on the kind and concentration of the impurities (for pure O_2 and solid solutions containing 0.34% N_2 the jump amounts to ~2/3 of the total thermal conductivity; ~2/5 in O_2–0.94% N_2; and ~1/3 in O_2–1% Ar), the thermal conductivity jump appears to be an intrinsic property of the $\alpha-\beta$ transition.

There is a reason to believe that the thermal conductivity jump at the $\alpha-\beta$ transition and the insensitivity of the thermal conductivity of the β phase to the presence of impurities have a common origin, namely, peculiar features of the β phase. As it was recently demonstrated in an x-ray investigation [18], a strong spontaneous magnetostriction is characteris-

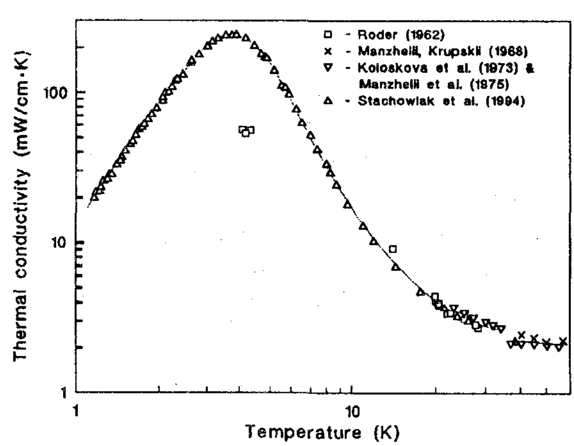

Fig. 5. Thermal conductivity of solid nitrogen as a function of temperature.

tic of this phase. It leads to a considerable inhomogeneous lattice distortion. This distortion contributes to the thermal resistivity so significantly that scattering on impurities turns out to be just a small additional contribution.

Therefore, the data obtained suggest that our previous statement (see [3]) that the thermal conductivity jump at the $\alpha-\beta$ transition is connected entirely with the magnon contribution to the heat flow should be revised. The quantity that undergoes the jump at the transition point is rather the phonon mean free path. It may be suggested that the drop in the phonon mean free path is due to a new scattering factor emerging here, viz. the regions of inhomogeneous lattice distortion caused by the strong magnetostriction effects, inherent in the β phase of solid oxygen. But only thermal conductivity measurements in a strong magnetic field will make it possible to separate unambiguously the contributions of the two effects in the jump.

4. Solid nitrogen

The thermal conductivity of solid nitrogen have been so far studied from the triple point down to 20 K. Roder [6] measured the thermal conductivity of $\alpha-N_2$ in the narrow temperature range 20–28 K with a relative error within 10%. The isolated points, measured at 4 and 14 K, are given with great errors. Manzhelii's group extended the measurements up to 57.5 K [5,7] (the relative error did not exceed 5%).

The sample growth method for solid nitrogen in this report was the same as for solid oxygen. Nuclei of the crystal were seeded from the liquid phase, the main part of the sample being grown directly from the gas phase. The growth rate of the crystal was about 1 mm/h. After crystallyzation, the samples were annealed for 12 h slightly below the triple point of nitrogen and then cooled to liquid helium temperature, the cooling rate for both the β and α phases being 1 K/h. The passing through the region of the $\beta-\alpha$ phase transition was realized in a time period of 16 h. As a result, the samples cooled down to liquid-helium temperature appeared to be transparent, without visible cracks and defects. The grain size, as estimated by observing the samples in polarized light, was about 3–4 mm. Among the parameters that influence sample quality, the most critical was the cooling rate in the region of the $\beta-\alpha$ transition. If the time of cooling was too short, the sample of the α phase contained a considerable amount of defects, which can be infered not only from visual inspection (opaqueness of the crystal) but also from a decrease of the thermal conduction. The measurements have been conducted by the stationary linear-flow method. The random error of the measurements at low temperatures did not exceed 1.5%, above 20 K it increased to 3%. The systematic error did not exceed 3%.

Measured thermal conductivities of solid nitrogen are shown in Fig. 5. The data of different authors in the temperature ranges where the measurements overlap agree within the errors specified in the publications. The temperature dependence of the thermal conductivity in the α phase is typical of dielectric crystals with a maximum around 3.6 K (the magnitude of κ at the maximum is approximately 250 mW/(cm·K)).

The results of the measurements were analyzed using the method of Callaway [9], taking into account the following mechanisms of phonon scattering: scattering on grain boundaries, on dislocation stress fields, on point defects, and three-phonon processes. Since the excitation energy even for the lowest libron branch is large enough, neither the contribution of librons to the heat transport nor the phonon-libron scattering were taken into consideration. As a result, the size of crystallites, the density of dislocations, and the density of point defects were estimated. The average dimension of crystallites ($4.4\cdot10^{-2}$ mm) turned out to be close to the value obtained for rare gas solids [20]. The difference between this value and the visual data can be explained by the existence in solid nitrogen of a subgrain structure observed earlier in rare gas solids [21]. The value obtained for the point-defect density (0.16%), though somewhat smaller, correlates with the natural content of the ^{15}N isotope.

A comparison of the thermal conductivity as a function of reduced temperature T/Θ_D (Θ_D is the Debye temperature) for solid nitrogen and oxygen is given in Fig. 6. This comparison reflects rather complex dinamics of these solids which includes the coupling between acoustic phonons, magnons, and librons in the case of solid oxygen, and acoustic and optical phonons and librons in the case of solid nitrogen. In particular, the fact that in the range

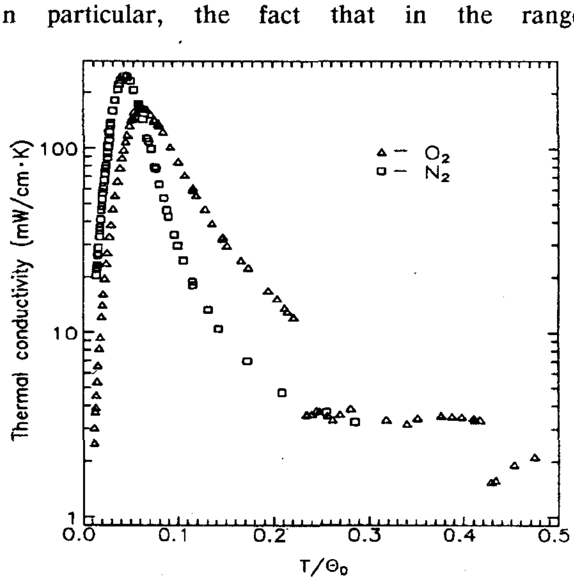

Fig. 6. Thermal conductivity of solid O_2 and N_2 vs. T/Θ_D.

$0.06 < T/\Theta_D < 0.2$ the thermal conductivity of N_2 decreases with temperature more rapidly is likely to reflect a contribution of optical phonon modes to scattering processes, which is absent in solid oxygen.

5. N_2-O_2 solid solutions

The N_2-O_2 phase diagram [14] is strongly asymmetric and the solubility of oxygen in solid nitrogen is considerably greater than that of nitrogen in solid oxygen. As a result, the effect of the oxygen impurity on the properties of the solid solutions can be studied in a wide concentration range.

As known, the triplet ground state of the oxygen molecule, $^3\Sigma_g^-$, is split into a singlet and doublet, the splitting being $D_0 = 5.71$ K [22] for the free particle (so-called spin-figure constant). On introduction of the oxygen molecule into the nitrogen matrix a quasilocal level appears at the low-energy side of the spectrum. As a result, low temperature anomalies can be observed in thermal properties of this crystal.

Papers [23–25] deal with the specific heat and thermal expansion of solid nitrogen containing oxygen impurities. The anomalies found in these works correspond satisfactorily to the Schottky curve with a doubly degenerate upper level and a splitting $D = 5.14$ K. The difference between D and D_0 results from the fact that the effective magnitude of the spin-figure interaction for the molecule embedded in the crystal is renormalized by the librational motion of the oxygen particle [26].

With increasing concentration of impurity molecules, an observable amount of clusters (exchange coupled molecules) appears. Their appearance affects the position and magnitude of the impurity anomalies since the magnetic spectrum of a cluster differs from that of a single molecule [27,28].

Contrary to the specific heat and thermal expansion phenomena, which are sensitive only to the position of the impurity levels, thermal conductivity is extremely sensitive to the broadening of the impurity levels. Hence, analysis of the thermal conductivity as a function of both concentration and temperature can provide considerable information on the rearrange-

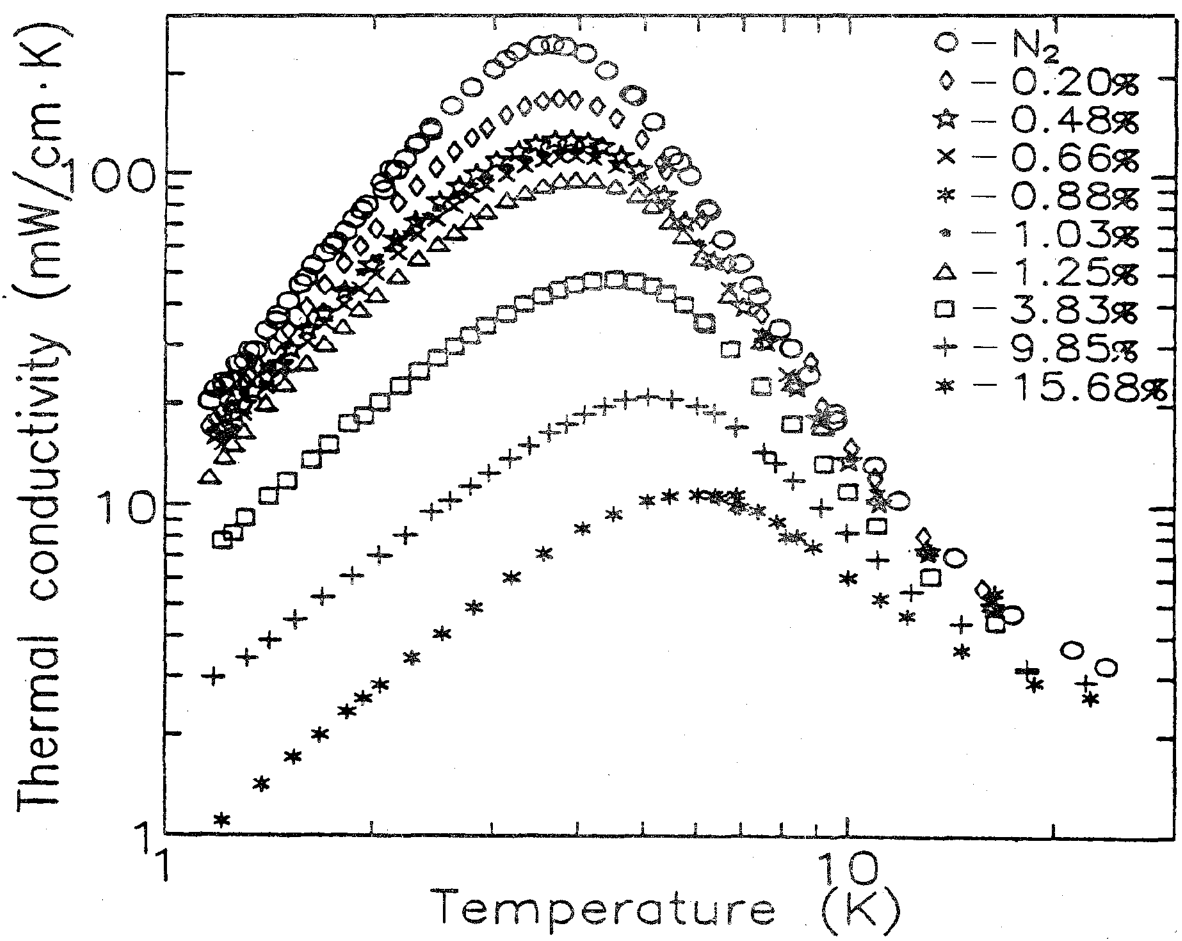

Fig. 7. Temperature dependencies of the thermal conductivity of the N_2-O_2 solid solutions for various concentration of O_2.

ment of the impurity spectrum. Such a rearrangement is predicted by the theory of disordered systems [29,30].

In this Section we report results of the first measurements of the thermal conductivity of N_2-O_2 solid solutions. The measurements were carried out in the O_2 fraction and temperature ranges $0 < c < 16\%$ and $1.2\ K < T < 20\ K$, respectively. The purity of the materials investigated were as follows: 99.99% oxygen (0.01% CO_2), 99.997% nitrogen (0.002% O_2). The gaseous mixtures for samples were prepared by the *PVT* method. The composition analysis of the samples was performed before and after measurements with the help of a mass spectrometer. The error of the composition determination did not exceed 0.01%. The samples were grown from the gas phase.

Temperature dependencies of the thermal conductivity coefficient $\kappa(T)$ of $(N_2)_{1-c}(O_2)_c$ solid solutions for various oxygen impurity concentrations c are presented in Fig. 7. For all the solid solutions examined the $\kappa(T)$ dependencies reveal a characteristic curve with a maximum. The influence of this impurity on the magnitude of the thermal conductivity is most

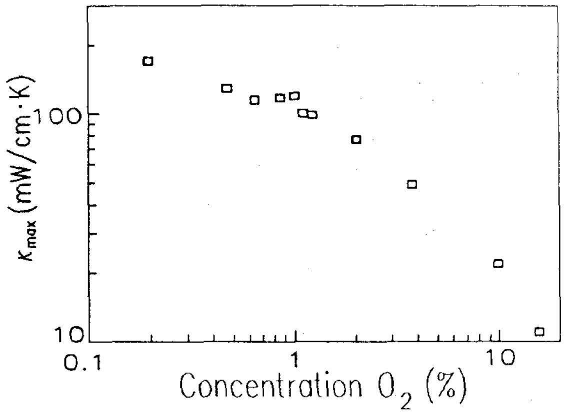

Fig. 8. The thermal conductivity at maximum, κ_{max}, versus O_2 concentrations.

distinct within the temperature range $T < T_{max}$, decreasing rapidly with increasing temperature at $T > T_{max}$. The magnitude, $\kappa_{max}(c)$, (Fig. 8) and position, $T_{max}(c)$, of the thermal conductivity maximum depend strongly on the O_2 concentration and exhibit a discontinuity at $c \sim 1\%$.

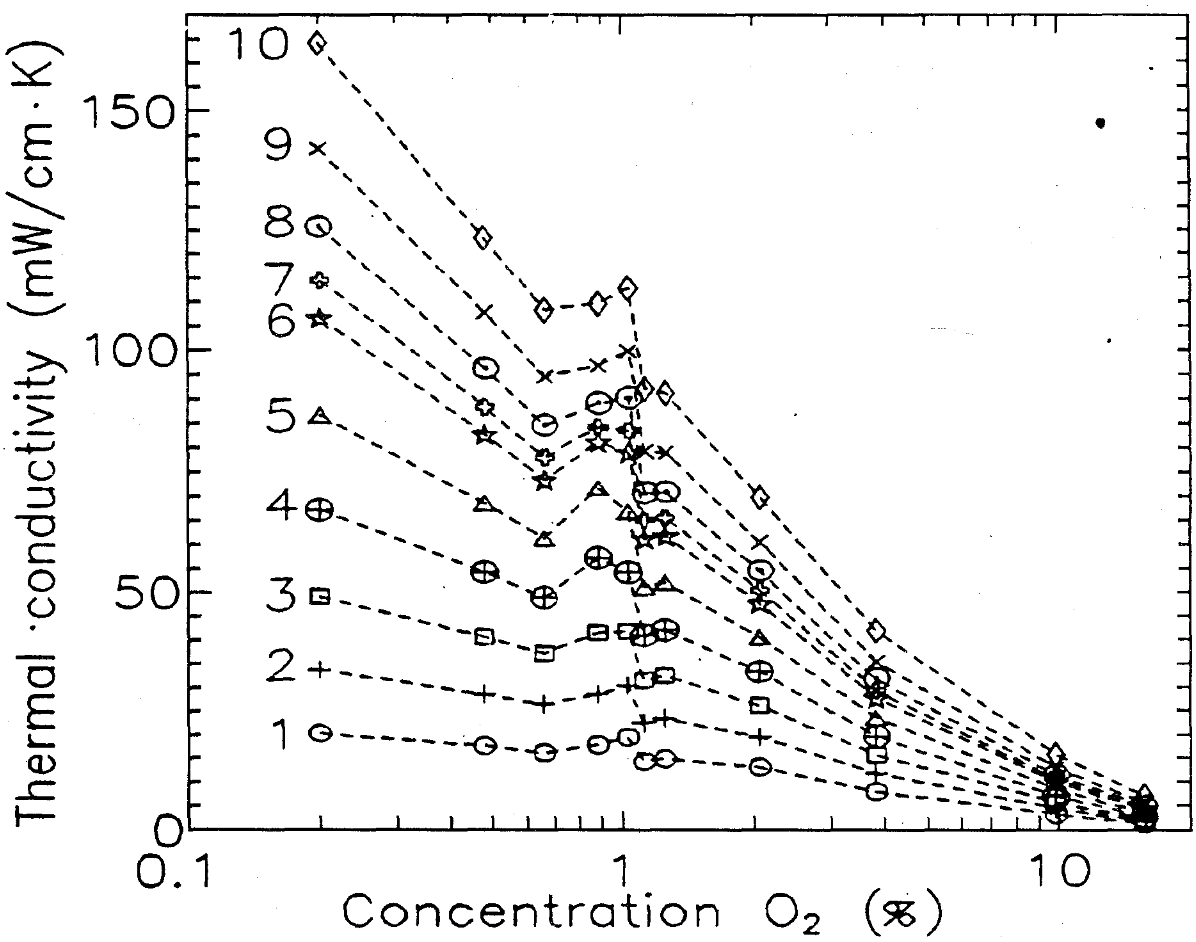

Fig. 9. Thermal conductivity of the N_2-O_2 solid solutions as a function of O_2 concentration at constant temperatures, K: 1.25 (*1*), 1.5 (*2*), 1.75 (*3*), 2.0 (*4*), 2.25 (*5*), 2.5 (*6*), 2.6 (*7*), 2.75 (*8*), 3.0 (*9*), 3.5 (*10*).

The dependence of the low temperature thermal conductivity on the O_2 concentration at various temperatures in the range $T < T_{max}$ (1.25–3.5 K) is shown in Fig. 9. Three different concentration ranges: (I) $c < 0.7\%$; (II) $0.7 < c < 1.1\%$; (III) $c > 1.1\%$ with different character of $\kappa(T)$ may be distinguished there.

In the range (I), all the curves can be satisfactorily described by a power law $\kappa(c, T = \text{const}) \sim c^{\alpha(T)}$. The exponent α depends on temperature and ranges from $-1/5$ to $-1/3$ for 1.25 and 3.5 K, respectively. Such a behavior of the thermal conductivity as a function of concentration suggests that there is a strong interference between the resonance scattering on impurities and the normal processes [31].

The variation of the thermal conductivity with concentration is more complex in the range (II). For temperatures $1.25\ \text{K} < T < 1.75\ \text{K}$ and $2.75\ \text{K} < T < 3.5\ \text{K}$ the dependencies $\kappa(c)$ are anomalous, i.e. the conductivity increases with increasing impurity concentration. Within the range $1.75\ \text{K} < T < 2.75\ \text{K}$, the $\kappa(c, T = \text{const})$ dependencies are nonmonotonic and a maximum appears at $c \sim 0.9\%$. The temperature dependencies of the thermal conductivity obtained for various O_2 concentrations exhibit a peculiarity, characteristic only of the system considered. The low temperature parts of the thermal conductivity versus temperature curves can be described by a power law of the type $\kappa(T, c = \text{const}) \sim T^{\beta(c)}$. The exponent β is a non-monotonous function of the oxygen impurity concentration (Fig. 10). It decreases from $\beta = 2.67$ for pure N_2 down to $\beta = 1.65$ for $c \sim 10\%$ and increases with further increase of c up to $\beta = 1.8$ at $c \sim 16\%$.

At temperatures above the maximum ($T > 3.5$ K), the anomalies in the $\kappa(c)$ dependencies disappear quite rapidly with increasing temperature, though they are still observable up to ~ 10 K.

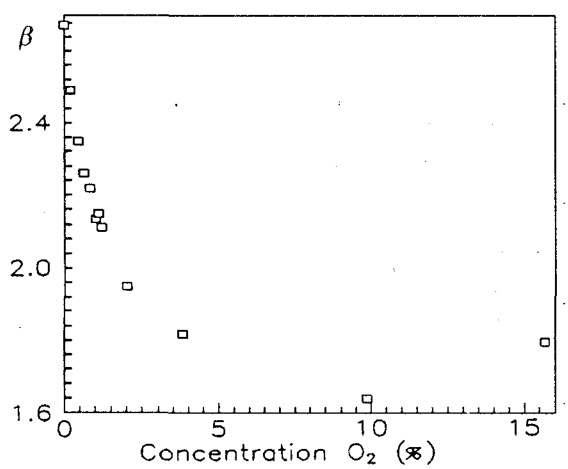

Fig. 10. Dependence of the exponent β of the power law $\kappa(T) \sim T^{\beta}$ describing the low temperature part of the thermal conductivity curves vs. the O_2 impurity concentration.

The simplest concentration dependence of the thermal conductivity is seen for the range III, where $\kappa(c, T = \text{const})$ is inveresely proportional to the O_2 concentration, and consequently the thermal resistivity is directly proportional to the O_2 concentration.

In the literature devoted to the thermal conductivity of insulators with paramagnetic impurities, the interpretation of experimental results is usually based on models that, in addition to the standard mechanisms leading to the heat resistivity, take into account the resonant phonon scattering by the quasi-local modes, associated with the spin or rotational degrees of freedom [32]. Another approach, formulated for the first time by Jacobsen and Stevens [30] assumes that the interaction of phonons with impurity spin levels leads to the creation of coupled spin-phonon modes. In this approach the observed anomalies can result from the resonant phonon scattering by the coupled spin-phonon modes.

Both theoretical approaches, which predict in fact the same result, viz. a decrease of the thermal conductivity of the crystals with the concentration of impurities, cannot explain the complex concentration dependence of the thermal conductivity of the N_2-O_2 solid solutions. At the same time a rather apparent assumption about the impurity-driven phase transition in this range of temperatures and impurity concentrations seems to be ruled out on the basis of x-ray [14,15], calorimetric [23,24], dilatometric [25] and other measurements performed on these solid solutions [16,17]. Moreover, even if the lattice transformation were energetically favorable, such a transition would be frozen out at such a low temperature.

We would like to propose another mechanism of the non-monotonic dependence of the thermal conductivity in the solids under discussion. As it will be discussed in detail elsewhere, coupled spin-phonon modes not only can present an additional source of thermal resistivity, but under certain conditions can contribute to the heat transport, comparably with the phonons.

Due to the spin-phonon coupling the sound velocity and the energy-momentum relation of spin degrees of freedom are renormalized. As a result, the phonon heat transport is decreased, but at the same time, an additional heat transport connected with the optical branch of the coupled spin-phonon spectrum appeares. The phonon contribution decreases roughly linearly with impurity concentration and the «optical» heat transport is quadratic in concentration at low impurity contents and tends to a concentration-independent contribution at larger concentrations. Thus, according to the mechanism proposed, the resulting thermal conductivity at constant temperature goes at first through a minimum and then through a maximum, in qualitative agreement with experiment.

Based on these considerations we think that the observable increase of the thermal conductivity in region (II) is associated with an extra contribution originating from the optical modes of the spin-phonon spectrum. We do not try to compare the calculated results with experiment because this would require a far more sophisticated theory. But we have demonstrated that the mechanism proposed may be responsible for the anomalies observed in the thermal conductivity.

As the impurity concentration increases further (range III), a considerable number of the exchange-coupled pairs of impurity molecules appears, having an entirely different spectrum [24–28]. This may lead to a rearrangement of the spin-phonon spectrum, strongly affecting the thermal conductivity.

6. Conclusions

In conclusion, we present results of measurements of the thermal conductivity of α, β, and γ phases of solid oxygen. A simple qualitative analysis is given to explain the anomalies observed: we attribute the jump in the thermal conductivity at the $\alpha-\beta$ transition to an anomalously high magnetostriction in the β phase; we ascribe the abnormally weak temperature dependence of the thermal conductivity in the beta phase to an anomaly in the temperature dependence of the sound velocities, and the increase in the thermal conductivity in the γ phase is associated with a weakening of the photon scattering by the hindered rotation and by the decrease of the short-range magnetic order with rising temperature.

We present results of measurements of the thermal conduictivity of solid nitrogen in the temperature range 1.2–38 K. The temperature dependence of the thermal conductivity reflects rather complex dynamics of the solid which includes the coupling between the acoustic and optical phonons and librons.

We present results of measurements of the thermal conductivity of solid oxygen doped with impurities of N_2 and Ar. It was shown that in the antiferromagnetic α phase at temperatures $T < 10$ K, doping with nonmagnetic impurities has a pronounced effect on the thermal conductivity. We suggest that in the low temperature range, nonmagnetic imputities suppress the magnon contribution to heat transport. The jump of the thermal conductivity at the $\alpha-\beta$ transition, found earlier in pure oxygen, survives in solid solutions. Thermal conductivity of the β phase turned out to be virtually insensitive to impurities. This fact demonstrates that it is the phonon mean free path that undergoes a jump at the transittion to the β phase.

It was found that the thermal conductivity of the N_2-O_2 solid solutions is a complex non-monotonic function of the oxygen concentration.

Acknowledgments

This work was supported in part by the Polish State Committee for Scientific Research (Grant 2 0388 91 01) and in part by International Science Foundation (Grants U9N000 and U9N200).

1. T. A. Scott, *Phys. Rep.* C27, 89 (1976).
2. I. N. Krupskii, V. A. Slusarev, and Yu. A. Freiman, in: *Cryocrystals*, B. I. Verkin and A. F. Prikhotko (eds.), Naukova Dumka, Kiev (1983) (in Russian).
3. A. Jeżowski, P. Stachowiak, V. V. Sumarokov, J. Mucha, and Yu. A. Freiman, *Phys. Rev. Lett.* **71**, 97 (1993).
4. P. Stachowiak, V. V. Sumarokov, J. Mucha, and A. Jeżowski, *Phys. Rev.* **B50**, 543 (1994).
5. V. G. Manzhelii and I. N. Krupskii (1968), in: *Physics of Condensed State*, Institute of Low Temperature Physics and Engineering, Kharkov, USSR (1968), vol. 2, p. 3 (in Russian).
6. H. M. Roder, *Cryogenics* 2, 302 (1962).
7. L. A. Koloskova, I. N. Krupskii, V. G. Manzhelii, and B. Ya. Gorodilov, *Fiz. Tverd. Tela* **15**, 1913 (1973) [*Sov. Phys. Solid State* **15**, 1278 (1973)]; V. G. Manzhelii, V. B. Kokshenev, L. A. Koloskova, and I. N. Krupskii, *Fiz. Nizk. Temp.* **1**, 1302 (1975) [*Sov. J. Low Temp. Phys.* **1**, 624 (1975).
8. A. F. Prikhotko, Yu. G. Pikus, and L. I. Shanskii, *Opt. Spektrosk.* **54**, 470 (1983) [*Opt. Spectrosc.* (USSR) **54**, 277 (1973)].
9. D. N. Batchelder, in: *Rare Gas Solids*, M. L. Klein and J. A. Venables (eds.), Academic, New York (1977).
10. N. N. Zholonko, B. Ya. Gorodilov, and A. I. Krivchikov, *Pis'ma Zh. Eksp. Teor. Fiz.* **55**, 174 (1992) [*JETP Lett.* **55**, 167 (1992)].
11. L. M. Tarasenko, in: *Thermophysical Properites of Substances and Materials* (1981), No 18, p. 72 [in Russian].
12. I. N. Krupskii, A. I. Prokhvatilov, Yu. A. Freiman, and A. I. Erenburg, *Fiz. Nizk. Temp.* **5**, 271 (1979) [*Sov. J. Low Temp. Phys.* **5**, 130 (1979)].
13. C. H. Fagerstroem and A. C. Hollis Hallett, *J. Low Temp. Phys.* **1**, 3 (1969).
14. A. S. Baryl'nik, A. I. Prokhvatilov, and L. D. Yantsevich, *Fiz. Nizk. Temp.* **15**, 501 (1989) [*Sov. J. Low Temp. Phys.* **15**, 282 (1989)].
15. A. I. Prokhvatilov and A. S. Baryl'nik, *Fiz. Nizk. Temp.* **11**, 1280 (1985) [*Sov. J. Low Temp. Phys.* **11**, 707 (1985)].
16. I. M. Pritula and L. V. Khashchina, *Fiz. Nizk. Temp.* **18**, 1035 (1992) [*Sov. J. Low Temp. Phys.* **18**, 727 (1992)].
17. I. M. Pritula, L. V. Khashchina, and I. Ya. Fugol, *Fiz. Nizk. Temp.* **18**, 761 (1992) [*Sov. J. Low Temp. Phys.* **18**, 539 (1992)].
18. A. S. Baryl'nik and A. I. Prokhvatilov, *Fiz. Nizk. Temp.* **20**, 912 (1994) [*Low Temp. Phys.* **20**, 716 (1994)].
19. J. Callaway, *Phys. Rev.* **113**, 1046 (1959).
20. R. M. Kimber and S. J. Rogers, *J. Phys.* C6, 2279 (1973).
21. D. N. Batchelder, D. L. Losee, and R. O. Simmons, *J. Phys. Chem. Solids* 28, suppl., 843 (1967).
22. M. Tinkham and M. W. P. Stranberg, *Phys. Rev.* 97, 937 (1955).
23. J. C. Burford and G. M. Graham, *J. Chem. Phys.* **49**, 763 (1968).
24. V. V. Sumarokov, Yu. A. Freiman, V. G. Manzhelii, and V. A. Popov, *Sov. J. Low Temp. Phys.* 6, 580 (1980).
25. A. Jeżowski, Yu. A. Freiman, A. M. Tolkachev, V. P. Azarenkov, V. G. Manzhelii, and E. A. Kosobutskaya, *Sov. J. Low Temp. Phys.* 6, 723 (1980).

26. Yu. A. Freiman and A. Jeżowski, *Sov. J. Low Temp. Phys.* **10**, 340 (1984).
27. Yu. A. Freiman, A. Jeżowski, and V. V. Sumarokov, *J. Phys.* **C19**, 5309 (1986).
28. V. S. Ostrovkii, V. V. Sumarokov, and Yu. A. Freiman, *Sov. J. Low Temp. Phys.* **12**, 116 (1986).
29. M. A. Ivanov, V. M. Loktev, and Yu. A. Pogorelov, *Phys. Rep.* **C51**, 209 (1987).
30. M. A. Ivanov, V. M. Loktev, and Yu. A. Pogorelov, *Sov. J. Low Temp. Phys.* **10**, 340 (1984).
31. T. N. Antsygina and V. A. Slusarev, *Low Temp. Phys.* **19**, 348 (1993).
32. R. O. Pohl, *Phys. Rev. Lett.* **8**, 481 (1962).
33. E. H. Jacobsen and K. W. H. Stevens, *Phys. Rev.* **131**, 1976 (1963).